frontiers in Environmental Science

ORIGINAL RESEARCH
published: 17 July 2020
doi: 10.3389/fenvs.2020.00108

Radium Mass Balance Sensitivity Analysis for Submarine Groundwater Discharge Estimation in Semi-Enclosed Basins: The Case Study of Long Island Sound

Joseph Tamborski[1,2,3], J. Kirk Cochran[4], Henry Bokuniewicz[4], Christina Heilbrun[4], Jordi Garcia-Orellana[5,6], Valentí Rodellas[5] and Robert Wilson[4]*

[1] Department of Geosciences, Stony Brook University, Stony Brook, NY, United States, [2] Department of Marine Chemistry & Geochemistry, Woods Hole Oceanographic Institution, Woods Hole, MA, United States, [3] Centre for Water Resources Studies, Dalhousie University, Halifax, NS, Canada, [4] School of Marine and Atmospheric Sciences, Stony Brook University, Stony Brook, NY, United States, [5] ICTA, Institut de Ciència i Tecnologia Ambientals, Universitat Autònoma de Barcelona, Bellaterra, Spain, [6] Department de Física, Universitat Autònoma de Barcelona, Bellaterra, Spain

OPEN ACCESS

Edited by:
Makoto Taniguchi, Research Institute for Humanity and Nature, Japan

Reviewed by:
Vhahangwele Masindi, Council for Scientific and Industrial Research (CSIR), South Africa
Henrietta Dulai, University of Hawai'i at Mānoa, United States

***Correspondence:**
Joseph Tamborski
jtamborski@whoi.edu

Specialty section:
This article was submitted to Water and Wastewater Management, a section of the journal Frontiers in Environmental Science

Received: *13 June 2019*
Accepted: *23 June 2020*
Published: *17 July 2020*

Citation:
Tamborski J, Cochran JK, Bokuniewicz H, Heilbrun C, Garcia-Orellana J, Rodellas V and Wilson R (2020) Radium Mass Balance Sensitivity Analysis for Submarine Groundwater Discharge Estimation in Semi-Enclosed Basins: The Case Study of Long Island Sound. Front. Environ. Sci. 8:108. doi: 10.3389/fenvs.2020.00108

Estimation of submarine groundwater discharge (SGD) to semi-enclosed basins by Ra isotope mass balance is herein assessed. We evaluate ^{224}Ra, ^{226}Ra, and ^{228}Ra distributions in surface and bottom waters of Long Island Sound (CT-NY, United States) collected during spring 2009 and summer 2010. Surface water and bottom water Ra activities display an apparent seasonality, with greater activities during the summer. Long-lived Ra isotope mass balances are highly sensitive to boundary fluxes (water flux and Ra activity). Variation (50%) in the ^{224}Ra, ^{226}Ra, and ^{228}Ra offshore seawater activity results in a 63–74% change in the basin-wide ^{226}Ra SGD flux and a 58–60% change in the ^{228}Ra SGD flux, but only a 4–9% change in the ^{224}Ra SGD flux. This highlights the need to accurately constrain long-lived Ra activities in the inflowing and outflowing water, as well as water fluxes across boundaries. Short-lived Ra isotope mass balances are sensitive to internal Ra fluxes, including desorption from resuspended particles and inputs from sediment diffusion and bioturbation. A 50% increase in the sediment diffusive flux of ^{224}Ra, ^{226}Ra, and ^{228}Ra results in a ∼30% decrease in the ^{224}Ra SGD flux, but only a ∼6–10% decrease in the ^{226}Ra and ^{228}Ra SGD flux. When boundary mixing is uncertain, ^{224}Ra is the preferred tracer of SGD if sediment contributions are adequately constrained. When boundary mixing is well-constrained, ^{226}Ra and ^{228}Ra are the preferred tracers of SGD, as sediment contributions become less important. A three-dimensional numerical model is used to constrain boundary mixing in Long Island Sound (LIS), with mean SGD fluxes of $1.2 \pm 0.9 \times 10^{13}$ L y^{-1} during spring 2009 and $3.3 \pm 0.7 \times 10^{13}$ L y^{-1} during summer 2010. The SGD flux to LIS during summer 2010 was one order of magnitude greater than the freshwater inflow from the Connecticut River. The maximum marine SGD-driven N flux is $14 \pm 11 \times 10^{8}$ mol N y^{-1} and rivals the N load of the Connecticut River.

Keywords: radium isotopes, submarine groundwater discharge, porewater exchange, nitrogen, Long Island Sound

INTRODUCTION

Submarine groundwater discharge (SGD) is a component of the hydrologic cycle and can act as an important vector for the transport of nutrients, carbon, trace elements, and pollutants to the coastal ocean (Moore, 2010; Knee and Paytan, 2011). SGD includes both terrestrial, meteorically-derived groundwater driven by a positive onshore hydraulic gradient and marine (i.e., saline) groundwater, driven by a variety of physical forcing mechanisms including density, tide, and wave driven flow (Santos et al., 2012). Naturally occurring radium isotopes are powerful tracers of SGD, as brackish groundwaters are typically enriched in dissolved Ra isotopes by several orders of magnitude over seawater (Swarzenski, 2007; Charette et al., 2008). The Ra quartet spans a wide range of half-lives (^{223}Ra = 11.4 d, ^{224}Ra = 3.66 d, ^{226}Ra = 1600 y, and ^{228}Ra = 5.75 y) and has thus been applied to trace and quantify inputs of SGD to the ocean on a variety of scales (Moore, 2010). For a given area, evaluation of the Ra source terms (e.g., rivers, particle desorption, diffusion, and bioirrigation), and Ra sinks (e.g., mixing, radioactive decay) can be used to quantify SGD. A Ra flux supplied by SGD is typically invoked to explain any imbalance between Ra sink and Ra source fluxes. Consequently, a SGD-driven Ra flux can be converted to a volumetric water flow with a proper characterization of the SGD endmember Ra activity. Multiple Ra isotopes are often used to quantify SGD; however, differences between short-lived and long-lived Ra isotope mass balances are often poorly constrained or not fully understood (Moore et al., 2006; Beck et al., 2007, 2008; Garcia-Solsona et al., 2008; Knee et al., 2016; Tamborski et al., 2017b).

Each Ra isotope is sensitive to different source and sink terms, reflecting the time-scale of a particular process with respect to the Ra isotope half-life. For example, short-lived ^{223}Ra and ^{224}Ra are more rapidly lost via radioactive decay, while long-lived ^{226}Ra and ^{228}Ra are not. Thus, the water column inventory of ^{223}Ra and ^{224}Ra must be well constrained to evaluate these short half-life tracers. Furthermore, flow paths of varying time-scales may have unique short-lived and long-lived Ra activities, and thus these isotopes may trace different SGD and porewater exchange flow paths (Rodellas et al., 2017). In addition, different geological matrices can have unique ratios of uranium (^{223}Ra, ^{226}Ra), and thorium (^{224}Ra, ^{228}Ra) series isotopes, thus enabling the identification of different geologic sources (Charette et al., 2008; Swarzenski, 2007).

This article synthesizes sediment, surface water, bottom water and groundwater Ra isotope data that has been previously collected in the semi-enclosed tidal estuary of Long Island Sound (LIS; Krishnaswami et al., 1982; Copenhaver et al., 1993; Turekian et al., 1996; Garcia-Orellana et al., 2014; Bokuniewicz et al., 2015; Tamborski et al., 2017a,b). In addition, we present new data on long-lived ^{226}Ra and ^{228}Ra, previously collected during 2009 and 2010. Here, we use short-lived ^{224}Ra and long-lived ^{226,228}Ra to quantify total SGD to LIS by mass balance. The main objective of this article is to evaluate the sensitivity of SGD estimated from Ra isotope mass balances. We evaluate Ra source and sink terms, and provide general recommendations on best-practices for Ra mass balances in semi-enclosed basins for future studies. We conclude with a revised estimate of SGD-driven NO_3^- loadings to LIS.

MATERIALS AND METHODS

Study Site

Long Island Sound is a tidal estuary bound by New York City at its western end, the southern shore of Connecticut at its northern boundary and the northern shore of Long Island (NY) at its southern boundary (**Figure 1**). At the beginning of the 20th century, urbanization, and pollution from the Metropolitan New York area led LIS to be nicknamed the "urban sea" (Koppelman et al., 1976; Latimer et al., 2013). Bottom-water hypoxia and eutrophication have been linked to excess nitrogen inputs from wastewater, sewage effluent, river inputs, and groundwater (NYSDEC and CTDEP, 2000). Indeed, Long Island's coastal embayments are vulnerable to excess nitrogen loading from submarine groundwater inputs (Bokuniewicz, 1980; Capone and Bautista, 1985). However, the volume of total SGD to LIS is not well known, despite increasing recognition of this important pollutant pathway.

The volume of terrestrial SGD to LIS from both Connecticut and New York shorelines is generally well constrained from hydrogeologic models (Buxton and Modica, 1992; Scorca and Monti, 2001; Suffolk County, 2015). Ra isotope mass balances in LIS' smaller embayment, Smithtown Bay (Bokuniewicz et al., 2015; Tamborski et al., 2017b), and for the entire LIS (Garcia-Orellana et al., 2014) all suggest that total SGD is dominated by marine groundwater inputs. Tamborski et al. (2017b) found that SGD within the first 200 m of the shoreline, determined from short-lived radionuclide mass balances, was up to ∼55% greater than SGD estimates determined from long-lived radionuclides and physical seepage meter measurements. To explain this difference, they suggested that wave and tidal circulation SGD flow paths captured short-lived radionuclide fluxes due to their faster regeneration rates within sediments, while these flow paths would not capture ^{226}Ra and ^{228}Ra. Interestingly, the total SGD flux to Smithtown Bay determined by Bokuniewicz et al. (2015) from ^{224}Ra, which includes inputs to the entire bay, was one to three orders of magnitude greater than the total SGD flux within the first 200 m of the shoreline. This led Tamborski et al. (2017b) to hypothesize that there may be additional, deeper SGD flow paths farther offshore in Smithtown Bay and LIS, from either the deeper Magothy aquifer or seawater circulation through offshore permeable sediments driven by density-forcing mechanisms, in addition to short-scale circulation fluxes driven by bioturbation and wave pumping.

Analytical Methods

Surface and deep-water samples from LIS were collected aboard the *R/V Seawolf* during 24–30 April 2009, 29 July–04 August 2009, and 03–12 August 2010. These samples, along with an analysis of the short-lived Ra isotopes, are described in Garcia-Orellana et al. (2014). Separately, groundwaters were collected from intertidal cluster wells from a coastal bluff and a barrier beach subterranean estuary, during spring and

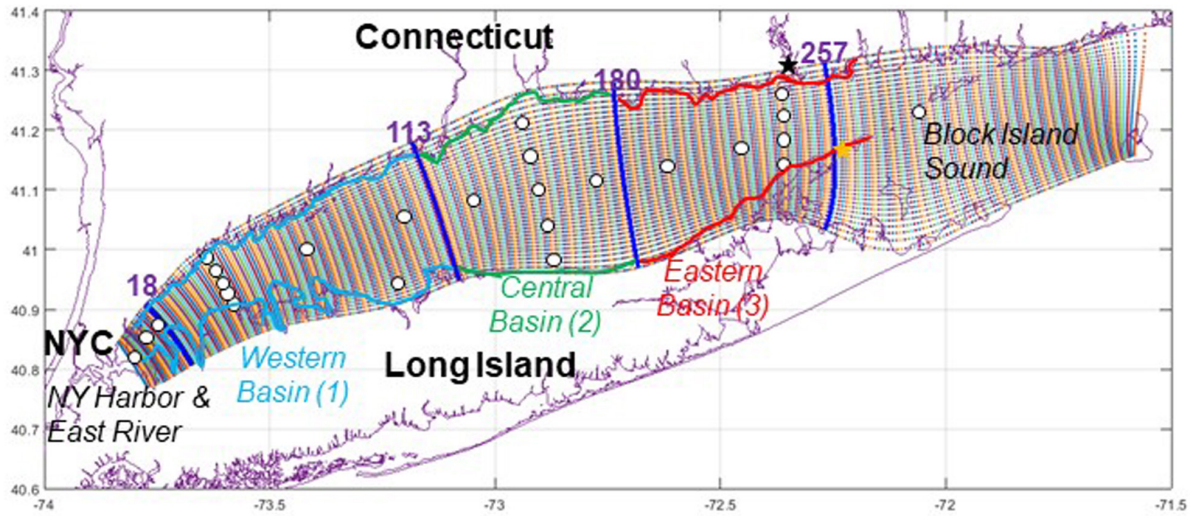

FIGURE 1 | The study site of Long Island Sound, bound between Long Island (NY), and Connecticut. Surface and bottom sampling stations are indicated by white circles. The mouth of the Connecticut River is indicated by a black star; Orient Point is indicated by an orange star. Long Island Sound is subdivided into the western (light blue), central (green), and eastern (red) basins, after Garcia-Orellana et al. (2014). Purple numbers correspond to the cross-section numbers in **Table 1**. Mean water exchange transports through cross-sections 18 113, 180, and 257 (N-S oriented dark blue lines) are derived from the three-dimensional model of Crowley (2005); the two-dimensional grid used in the model calculations is shown for reference and overlaps the land-ocean boundary.

summer 2014 and 2015. Additional coastal stations were sampled via drive-point piezometer at the low tide shoreline. These groundwater samples, including an analysis of the Ra quartet, are described in Tamborski et al. (2017a).

Briefly, water samples (seawater = 20–60 L; groundwater = 1–4 L) were filtered through MnO_2 impregnated acrylic fibers at a flow rate of <1 L min^{-1} to quantitatively extract dissolved Ra from solution onto the fiber. Short-lived ^{223}Ra and ^{224}Ra were measured using a Radium Delayed Coincidence Counter (RaDeCC; Moore and Arnold, 1996) immediately after sample collection. An additional count was performed 1 month after sample collection to measure ^{228}Th, to determine the amount of unsupported (excess) ^{224}Ra. Subsequently, the Mn-fibers were leached in a HCl and Hydroxylamine hydrochloride mixture and Ra was co-precipitated with $BaSO_4$. Precipitates were removed from the leachate, stored in glass vials and sealed for >3 weeks. Samples were counted on a Canberra Intrinsic Ge well detector, where the activity of long-lived ^{226}Ra and ^{228}Ra was determined from the 352 keV (^{214}Pb) and 911 keV (^{228}Ac) photopeaks, respectively. Gamma counting efficiencies were determined from NBS Standard Reference Material 4350B.

Estimates of Water Transport

LIS is made up of three basins (western, central, and eastern); water flux between basins and within LIS's boundaries were estimated to evaluate Ra mixing. Crowley (2005) determined that the transport through cross-sections to the west of Orient Point had a long term mean of 2.05×10^{13} L y^{-1} throughout the LIS basin (section 257; **Figure 1**), as determined from three-dimensional numerical simulations of circulation with meteorological and boundary sea-level forcing. The cross-sectionally-averaged transport exhibited significant temporal variability which was spatially coherent, with residence times on the order of several weeks to 2 months (Crowley, 2005). The differences in cross-sectionally-averaged transport can be attributed to localized effects of river discharge and to storage of water between sections. Water exchange fluxes were derived from the model of Crowley (2005) at cross-sections that approximately separate LIS into its three unique basins (western, central, and eastern; **Figure 1**) over a period between 2009 and 2010. Long term mean exchange transports through cross-sections exhibit an east to west net transport (**Table 1**). Note that these mean exchange transports have a standard error on the order of 10% because of the large temporal variability in the exchange. The mean surface freshwater inflow to the entire basin is on the order 1.34×10^{13} L y^{-1}, of which the Connecticut River at the far end of the Sound contributes approximately 1.19×10^{13} L y^{-1}, depending upon the seasonal conditions. The exchange transports at section 257 are corrected to accommodate the surface freshwater inflow between sections 18 and 257 (**Figure 1**). It should be noted that section 257 is located approximately at the longitudinal position of the Connecticut River, and that recent dye simulations emphasize that much of the Connecticut River waters exit to the east (Jia and Whitney, 2019).

RESULTS AND DISCUSSION

Ra Distribution

Long-lived ^{226}Ra and ^{228}Ra activities generally increased from east to west in LIS (**Table 2**). Compared to surface waters, deep-water Ra activities were greater on average for the western basin and similar to surface waters for the central and eastern basins (**Table 2**). Surface and deep-water Ra activities generally

TABLE 1 | Cross-sectional mean water exchange transports and standard error of the means, arranged by westerly flow (Qwest), and easterly flow (Qeast).

Cross-section #	$Q_{west} \pm SE \times 10^{14}$ L y^{-1}	$Q_{east} \pm SE \times 10^{14}$ L y^{-1}
18	0.65 ± 0.13	0.46 ± 0.12
113	3.14 ± 0.28	2.86 ± 0.28
180	3.46 ± 0.43	3.30 ± 0.39
257	5.95 ± 0.56	5.70 ± 0.50
257 (Corrected)	5.86 ± 0.56	5.80 ± 0.56

*Cross-section numbers correspond to the sections depicted on **Figure 1**.*

increased with decreasing salinity (**Figure 2**) and displayed an apparent seasonality, with greater activities during summer over spring (**Table 2** and **Figure 2**). During summer 2010, reduced bottom water salinity and elevated Ra activities suggest SGD was occurring several kilometers offshore.

Intertidal groundwater samples collected along the north-shore of Long Island (Tamborski et al., 2017a) spanned a wide salinity range (**Table 3**), with maximum Ra activities at a salinity of ∼18.6 (^{226}Ra = 106 dpm 100 L^{-1}; ^{228}Ra = 1650 dpm 100 L^{-1}; **Figure 2**). The mean (±standard deviation) ^{228}Ra/^{226}Ra activity ratio of Long Island marine groundwater was 7.5 ± 3.3 (salinity = 26.6 ± 1.0; n = 44). Marine groundwaters from the Connecticut shoreline had a ^{228}Ra/^{226}Ra activity ratio of 13.8 ± 4.1 (salinity = 28.4 ± 1.3; n = 5; **Table 3**). Connecticut fresh groundwaters, sampled from inland wells, had ^{228}Ra/^{226}Ra activity ratios between 0.2–1.4 (Krishnaswami et al., 1982; Copenhaver et al., 1993). This is in marked contrast to the ^{228}Ra/^{226}Ra activity ratio of the Connecticut River (∼3; Dion, 1983) and East River (3.8–4.1; Turekian et al., 1996). ^{228}Ra and ^{226}Ra activities of surface and bottom water samples, and activity ratios of possible sources, are presented in **Figure 3**.

Ra Mass Balance

Long-lived ^{226}Ra and ^{228}Ra mass balances for LIS were constructed after the short-lived ^{224}Ra mass balance developed by Garcia-Orellana et al. (2014) for spring 2009 and summer 2010, for the entire LIS basin. We have further developed Ra mass balances for each individual basin (western, central, and eastern; **Figure 1**). The Ra mass balances have been updated to reflect new terms, as described below. Briefly, a surface and deep box Ra inventory (dpm) is calculated for the western, central, and eastern basins of LIS (**Table 4**). The Ra inventory is calculated as the product of the water volume within each basin and the mean Ra activity of the basin. The Ra mass balance is written as:

$$J_{out} + J_{decay} = J_{in} + J_{river} + J_{desorp} + J_{diffusion} + J_{SGD} \quad (1)$$

Where the left-hand side represents Ra sinks and the right-hand side represents Ra sources. The Ra mass balance includes loss from mixing (J_{out}) and radioactive decay (J_{decay}). Ra sources include mixing (J_{in}), riverine input (J_{river}), the desorption of Ra from resuspended particles (J_{desorp}), molecular diffusion and bioturbation ($J_{diffusion}$), and SGD (J_{SGD}). Each term in Eq. 1 is assessed for ^{224}Ra, ^{226}Ra, and ^{228}Ra for the western, central, eastern, and total basins during spring 2009 and summer 2010, thus resulting in 24 unique Ra mass balances. All Ra mass balances are summarized in the **Supplementary Material** (**Supplementary Table S1**). Each term in Eq. 1 is described in further detail below, including a sensitivity analysis on the final estimated Ra flux supplied by SGD (section "Mass balance sensitivity").

Boundary Fluxes

Boundary fluxes determined from a three-dimensional numerical model (section "Estimates of water transport") are used to quantify the exchange of water and Ra isotopes between New York Harbor and the East River with the western basin of LIS (section 18), between the western basin and the central basin of LIS (section 113), between the central basin and the eastern basin of LIS (section 180), and between the eastern basin of LIS and Block Island Sound (section 257; **Table 1** and **Figure 1**). We use the same boundary flux for spring 2009 and summer 2010, although we acknowledge that there may be minor differences in seasonal water volume and thus exchange. Ra mixing fluxes (J_{in} and J_{out}) are calculated from the sectional mean water exchange transports and the associated endmember Ra activity. Because there is a net east to west water transport in LIS (**Table 1**), we use the mean deep-water Ra activities (**Table 2**) to represent Ra mixing from east to west. Mean Ra surface water activities (**Table 2**) are used to represent Ra mixing from west to east, for each respective basin under consideration. Boundary fluxes are summarized in **Figure 4**.

The ^{224}Ra, ^{226}Ra, and ^{228}Ra activities of the East River are, respectively, taken as 9 dpm 100 L^{-1} (Garcia-Orellana et al., 2014), 10.7 dpm 100 L^{-1} (Li et al., 1977), and 64 dpm 100 L^{-1} (Turekian et al., 1996) for both seasons. Block Island Sound seawater was previously sampled for long-lived Ra at 5 m and 25 m depth during summer 1991 (St101; Turekian et al., 1996). This same station was sampled during spring 2009 in this study. We use a ^{224}Ra, ^{226}Ra, and ^{228}Ra activity of 3.6, 5.3, and 29 dpm 100 L^{-1}, respectively, for spring 2009 and activities of 3.6, 8.5, and 47 dpm 100 L^{-1}, respectively, for summer 2010. It is important to note that only one sample is used to characterize the Ra endmember for each of these mixing input terms.

The Connecticut River is the largest river entering LIS. Connecticut River discharge was estimated as the mean discharge over the two-week period preceding each seasonal LIS survey, based on the average residence time of the eastern basin (Crowley, 2005). The Connecticut River discharge is taken as 2.52 × 10^{13} L y^{-1} during spring 2009 and 0.68 × 10^{13} L y^{-1} during summer 2010 from the USGS gaging station at Middle Haddam (ID 01193050). Note that the spring 2009 and summer 2010 Connecticut River discharges were, respectively, above and below the mean annual river discharge (∼1.2 × 10^{13} L y^{-1}). The Connecticut River is only considered in the eastern basin and total basin Ra mass balances. Several other rivers enter LIS from both Long Island (e.g., Nissequogue River) and Connecticut (e.g., Housatonic River, Thames River) shorelines, which together account for a cumulative discharge on the order of ∼0.4 × 10^{13} L y^{-1} (Koppelman et al., 1976); here we assume that one third of this water flux enters each of the three LIS basins. The riverine Ra flux to LIS (J_{river}) is calculated as the product of the river discharge to each basin and the dissolved Ra

TABLE 2 | Mean ^{226}Ra and ^{228}Ra activities in the three basins of Long Island Sound during spring 2009, summer 2009, and summer 2010, arranged by surface and deep-water samples.

	^{226}Ra Surface	^{228}Ra Surface	*n* (surface)	^{226}Ra Deep	^{228}Ra Deep	*n* (deep)
	(dpm 100 L^{-1})			(dpm 100 L^{-1})		
Spring 2009						
Western Basin	9.3 ± 1.4	61 ± 12	9	10.1 ± 1.3	71 ± 7	7
Central Basin	10.0 ± 0.8	58 ± 4	7	10.0 ± 0.9	52 ± 9	6
Eastern Basin	7.3 ± 1.9	39 ± 19	6	6.6 ± 1.3	33 ± 13	5
Mean	9.0 ± 1.8	54 ± 16	22	9.0 ± 2.0	54 ± 18	18
Summer 2009						
Western Basin	12.9 ± 3.2	97 ± 21	4	14.1 ± 1.2	104 ± 7	4
Central Basin	9.8 ± 1.3	57 ± 19	3	9.8 ± 1.4	56 ± 11	3
Eastern Basin	9.2 ± 0.6	50 ± 4	4	9.6 ± 0.6	41 ± 9	4
Mean	10.7 ± 2.7	69 ± 26	11	11.3 ± 2.4	68 ± 29	11
Summer 2010						
Western Basin	11.5 ± 2.6	80 ± 22	7	14.1 ± 0.6	98 ± 12	6
Central Basin	11.1 ± 0.7	73 ± 9	6	11.9 ± 1.4	72 ± 11	6
Eastern Basin	10.0 ± 1.3	69 ± 12	5	9.8 ± 0.9	48 ± 6	5
Mean	10.9 ± 1.9	75 ± 17	18	12.1 ± 2.0	74 ± 23	17

activity of the Connecticut River mouth (**Figure 1**). Surface water salinity at the station sampled near the mouth of the Connecticut River was ∼28; therefore, the Ra flux estimated here intrinsically includes the desorption of Ra from suspended riverine particles. This calculation assumes that the Ra endmember at the mouth of the Connecticut River is representative of all rivers entering LIS, as done by Turekian et al. (1996); riverine fluxes are summarized in **Figure 4**.

Internal Fluxes

The desorption of long-lived ^{226}Ra and ^{228}Ra from resuspended particles (J_{desorp}) throughout LIS is negligible due to the slow regeneration time of ^{226}Ra and ^{228}Ra in sediments. The desorption of ^{224}Ra is estimated from suspended particle concentrations for spring 2009 (1.5 ± 1.3 mg L^{-1}) and summer 2010 (4.0 ± 2.5 mg L^{-1}), and a surface-exchangeable ^{224}Ra activity of 0.75 dpm g^{-1}. Desorption of ^{224}Ra from tidally resuspended particles is 1.6 ± 1.4 × 10^4 dpm m^{-2} y^{-1} for spring 2009 and 4.4 ± 2.7 × 10^4 dpm m^{-2} y^{-1} for summer 2010 (Garcia-Orellana et al., 2014; **Figure 4**).

Sediment diffusion and bioturbation have been shown to be an important source of short-lived Ra isotopes to LIS, due to their relatively rapid regeneration rates within sediments (Garcia-Orellana et al., 2014). This source term should be relatively less important for the long-lived Ra isotopes, due to their slower regeneration rates in sediments. Tamborski et al. (2017b) conducted sediment core incubation experiments (at 20°C and 3°C; oxic, and hypoxic conditions) to determine the sediment flux of long-lived Ra isotopes for a sandy (intertidal) core and a silty (offshore) core from LIS. ^{228}Ra sediment fluxes in LIS were previously determined from the disequilibrium between solid-phase ^{228}Ra and its parent ^{232}Th (Cochran, 1979; Turekian et al., 1996), which integrates over several half-lives of ^{228}Ra and thus represents a mean-annual ^{228}Ra flux. Each of these methods includes a Ra flux from both molecular diffusion and bioirrigation. These various flux estimates were averaged together for coarse-grained sediments and fine-grained sediments. Fluxes were further separated by temperature (warm = summer; cold = early spring) and oxygen content (hypoxic = summer; oxic = early spring) to differentiate between spring and summer conditions (**Table 5**). Sediment-mediated ^{228}Ra and ^{226}Ra inputs were calculated using a LIS bottom surface area of 0.90 × 10^9 m^2, 1.08 × 10^9 m^2, and 0.96 × 10^9 m^2 for the western, central and eastern basins. Further, we assume a fine-grained and coarse-grained surficial sediment distribution for the western (70% fine, 30% coarse), central (50% fine, 50% coarse), and eastern (0% fine, 100% coarse) basins following Poppe et al. (2000). Sediment Ra fluxes are summarized in **Figure 4**.

Assuming steady-state, the radioactive decay of ^{224}Ra and ^{228}Ra is calculated as the product of the respective Ra inventory for each basin and the Ra isotope decay constant (0.189 d^{-1} for ^{224}Ra and 0.121 y^{-1} for ^{228}Ra). Decay of ^{226}Ra is negligible due to its long half-life (**Figure 4**). The excess Ra inventory in each basin (Σ Ra sinks – Σ Ra sources; Eq. 1) is presumed to be balanced by SGD (J_{SGD}). A negative SGD flux implies either that Ra sources approximately balance Ra sinks (within the propagated uncertainties), or that one (or more) known Ra flux is improperly characterized. SGD-derived Ra fluxes are converted into volumetric water flows by dividing the Ra flux by the Ra activity of the SGD endmember, sampled from intertidal wells and shoreline piezometer stations along both NY and CT shorelines (Garcia-Orellana et al., 2014; Tamborski et al., 2017a). Selection of the SGD Ra endmember is discussed below (section "SGD volumetric water flow to Long Island Sound").

Mass Balance Sensitivity

Analysis of Ra sources and sinks reveals that boundary fluxes dominate the long-lived Ra isotopes while sediment contributions (diffusion and desorption) and radioactive decay

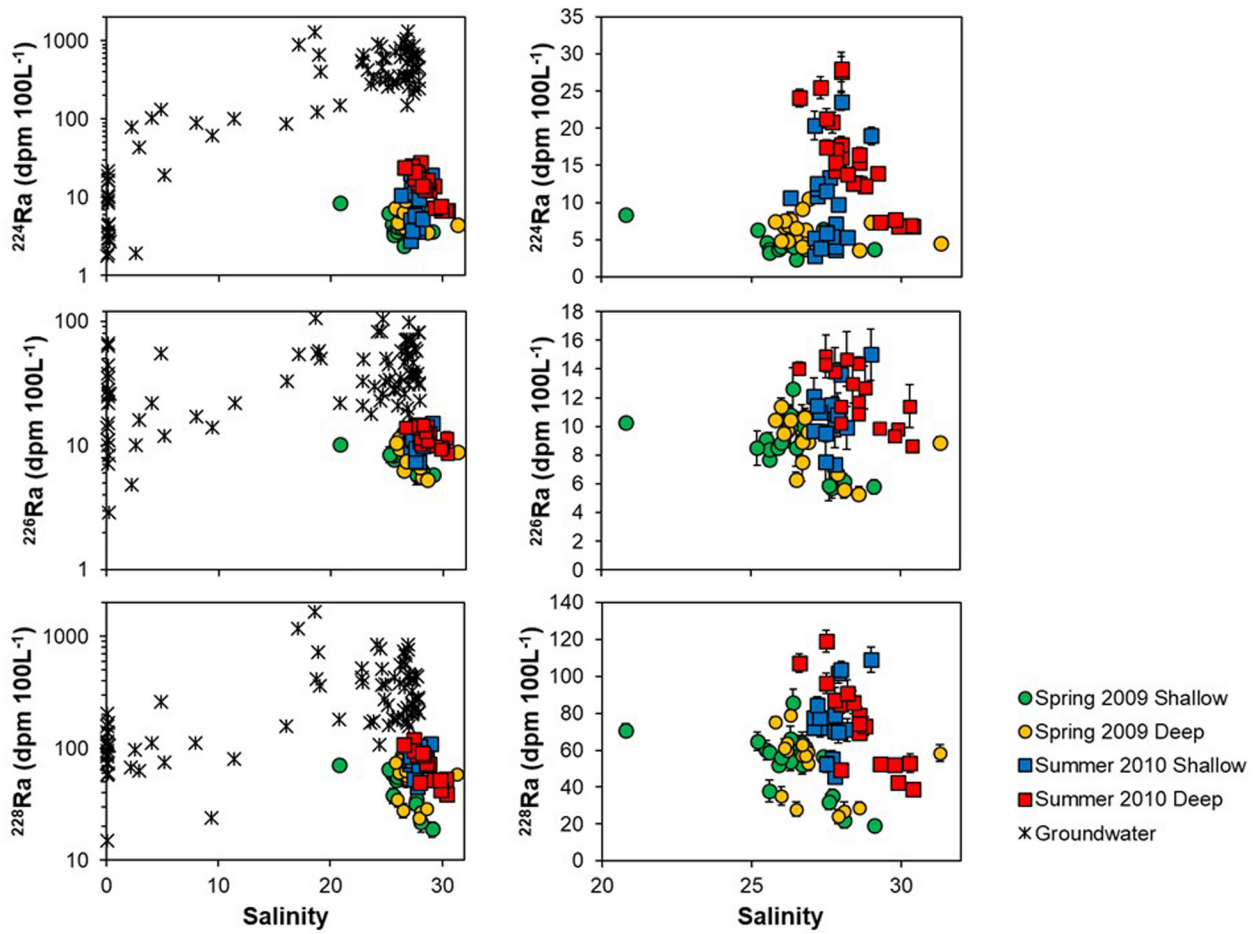

FIGURE 2 | Dissolved Ra vs salinity for Long Island Sound surface waters, bottom waters, and groundwaters. Surface and bottom water samples are presented in the right-hand panels for improved visualization and are arranged by season, from Garcia-Orellana et al. (2014). Groundwater samples are from intertidal cluster wells and shoreline piezometer stations on Long Island (Tamborski et al., 2017a) and Connecticut (Garcia-Orellana et al., 2014).

TABLE 3 | Summary of groundwater Ra endmembers from Long Island (LI) and Connecticut (CT) shorelines.

Groundwater source	Salinity	^{224}Ra dpm 100 L^{-1}	^{226}Ra dpm 100 L^{-1}	^{228}Ra dpm 100 L^{-1}	^{228}Ra/^{226}Ra	*n*
LI fresh groundwater*	0.1 ± 0.0	8 ± 6	25 ± 18	104 ± 45	6.2 ± 5.0	17
LI brackish groundwater*	15.5 ± 8.4	346 ± 340	36 ± 26	359 ± 390	9.0 ± 5.1	27
LI marine groundwater*	26.6 ± 1.0	523 ± 260	47 ± 21	344 ± 177	7.5 ± 3.3	44
CT fresh groundwaterˆ	<1	n/a	44 ± 36	27 ± 17	0.8 ± 0.5	7
CT marine groundwaterˆˆ	28.4 ± 1.3	356 ± 45	28 ± 8	381 ± 123	13.8 ± 4.1	5

*Groundwater samples are classified by salinity: fresh groundwater = 0–1; brackish groundwater = 4–24; and marine groundwater = 25–28. Error bars indicate ± 1 standard deviation from the mean. Note that brackish groundwaters from Connecticut are not included in this analysis. *Groundwaters from Tamborski et al. (2017a). ˆGroundwaters from Copenhaver et al. (1993) and Krishnaswami et al. (1982). ˆˆGroundwaters from Garcia-Orellana et al. (2014) and analyzed in this study.*

dominate the short-lived Ra isotopes (**Figure 4**). Ra mass balance sensitivity to each of these terms is discussed below.

Sediment diffusion, bioirrigation, and desorption support ∼50% of the ^{224}Ra inventory for LIS but only ∼6% of the ^{226}Ra inventory and ∼10–20% of the ^{228}Ra inventory (**Figure 4**). The ^{224}Ra sediment flux is constrained from sediment incubation experiments from five different locations (Garcia-Orellana et al., 2014); the ^{228}Ra sediment flux is constrained from four sediment incubations and two estimates from ^{228}Ra:^{232}Th disequilibrium (Cochran, 1979; Turekian et al., 1996). Is this representative of the entirety of LIS? Few Ra-based SGD studies capture sediment-mediated Ra inputs from more than a few measurements (Beck et al., 2007, 2008; Garcia-Solsona et al., 2008; Rodellas et al., 2012, 2015; Cai et al., 2014; Tamborski et al., 2017b).

The molecular diffusive flux of Ra from shallow porewater to overlying seawater is governed by the Ra concentration gradient between porewater and seawater (Fick's first law). Bioturbation and bioirrigation can further facilitate Ra transport by enhancing the effective sediment surface-area, thus complicating diffusive flux estimates. Due to its short half-life, ^{224}Ra regenerates rapidly in sediments from the decay of its particle-reactive parent ^{228}Th. The activity of ^{230}Th and ^{232}Th (the parents of ^{226}Ra and ^{228}Ra) are similar in LIS sediments, resulting in similar production rates in muddy and sandy sediments (Cochran, 1979). Therefore, seasonal redox changes may affect the diffusive flux of short-lived and long-lived Ra isotopes differently, as the redox interface migrates between bottom waters and the shallow subsurface (Garcia-Orellana et al., 2014). This seasonal control impacts Ra diffusion and more importantly, the influence of the benthic fauna, which are presumed to be less active during colder periods. We have attempted to capture this variability by using different sediment incubations for spring and summer conditions (**Table 5**).

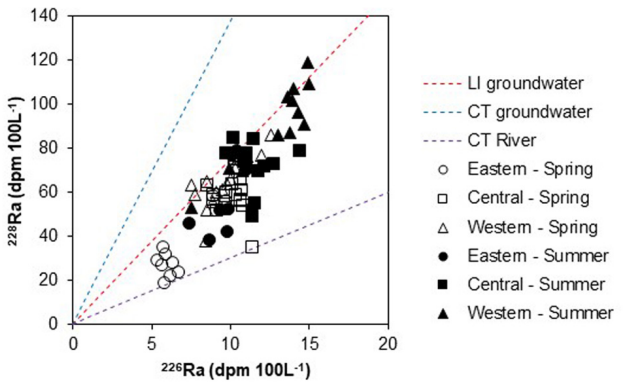

FIGURE 3 | Cross-plot of ^{228}Ra and ^{226}Ra activities in shallow and deep waters collected from Long Island Sound, arranged by sampling season. Note that error bars are generally smaller than the symbol size. Dashed lines indicate the ^{228}Ra/^{226}Ra activity ratio of possible Ra sources. Data sources: Connecticut River (AR = 3; Dion, 1983); Connecticut marine groundwater (AR = 14 ± 4; this study); and Long Island marine groundwater (AR = 8 ± 3; Tamborski et al., 2017a).

Are the incubations used to quantify diffusion and bioirrigation from sediments accurate? ^{228}Ra fluxes for muddy LIS sediments, determined from the deficit of solid-phase ^{228}Ra relative to its parent ^{232}Th (Cochran, 1979; Turekian et al., 1996), are in general agreement with ^{228}Ra fluxes determined from sediment chamber incubations (33–82 dpm m^{-2} d^{-1} vs 12–207 dpm m^{-2} d^{-1}). The solid-phase ^{228}Ra:^{232}Th approach integrates over the half-life of ^{228}Ra, therein representing a mean-annual ^{228}Ra flux; therefore, these estimates seem reasonable at the seasonal time-scale considered here. A recent study found the traditional sediment incubation approach for ^{224}Ra flux determination to be similar to ^{224}Ra fluxes determined from ^{224}Ra:^{228}Th disequilibrium (Shi et al., 2018). Thus, it seems that the incubations used to quantify the Ra flux from diffusion and bioirrigation are accurate, although it remains to be seen how representative these several cores are for the entirety of LIS. A 50% increase in the diffusive flux of ^{224}Ra, ^{226}Ra, and ^{228}Ra, while keeping all other parameters equal (Eq. 1), results in a ∼30% decrease

TABLE 4 | ^{226}Ra (top) and ^{228}Ra (bottom) inventories in western, central and eastern LIS in spring 2009 and summer 2010.

	Basin	Water volume (×10^{12} L)	Spring 2009		Summer 2010	
			Mean ^{226}Ra activity (dpm 100 L^{-1})	^{226}Ra inventory (×10^{11} dpm)	Mean ^{226}Ra activity (dpm 100 L^{-1})	^{226}Ra inventory (×10^{11} dpm)
Surface	Eastern basin	3.40	7.3 ± 1.9	2.5 ± 0.7	10.0 ± 1.3	3.4 ± 0.5
	Central basin	2.90	10.0 ± 0.8	2.9 ± 0.2	11.1 ± 0.7	3.2 ± 0.2
	Western basin	1.87	9.3 ± 1.4	1.8 ± 0.3	11.5 ± 2.6	2.1 ± 0.5
Deep	Eastern basin	18.8	6.6 ± 1.3	12.3 ± 2.4	9.8 ± 0.9	18.5 ± 1.7
	Central basin	17.6	10.0 ± 0.9	17.7 ± 1.5	11.9 ± 1.4	20.9 ± 2.4
	Western basin	7.42	10.1 ± 1.3	7.5 ± 1.0	14.1 ± 0.6	10.5 ± 0.5
Total		52.0		45 ± 3		59 ± 3
			Spring 2009		Summer 2010	
			Mean ^{228}Ra activity (dpm 100 L^{-1})	^{228}Ra inventory (×10^{12} dpm)	Mean ^{228}Ra activity (dpm 100 L^{-1})	^{228}Ra inventory (×10^{12} dpm)
Surface	Eastern basin	3.40	39.2 ± 18.6	1.3 ± 0.6	68.9 ± 11.9	2.3 ± 0.4
	Central basin	2.90	58.5 ± 4.2	1.7 ± 0.1	73.2 ± 9.0	2.1 ± 0.3
	Western basin	1.87	61.4 ± 12.5	1.2 ± 0.2	80.1 ± 22.4	1.5 ± 0.4
Deep	Eastern basin	18.8	33.3 ± 12.7	6.3 ± 2.4	47.7 ± 6.0	9.0 ± 1.1
	Central basin	17.6	52.4 ± 9.0	9.2 ± 1.6	71.7 ± 11.1	12.6 ± 2.0
	Western basin	7.42	70.8 ± 7.2	5.3 ± 0.3	97.7 ± 11.8	7.3 ± 0.9
Total		52.0		25 ± 3		35 ± 3

TABLE 5 | Summary of ^{226}Ra and ^{228}Ra sediment fluxes in Long Island Sound.

Season	Sediment conditions	^{226}Ra (dpm m^{-2} d^{-1})	^{228}Ra (dpm m^{-2} d^{-1})
Spring	Fine-grained Oxic	28 ± 14	207 ± 104
	Coarse-grained Cold	3 ± 2	16 ± 8
Summer	Fine-grained Hypoxic	1 ± 1	42 ± 26*
	Coarse-grained Warm	8 ± 4	39 ± 20

*^{224}Ra fluxes were determined for each LIS basin and are summarized in Garcia-Orellana et al. (2014). Data Sources: Tamborski et al. (2017b); *Average of Cochran (1979); Turekian et al. (1996), and Tamborski et al. (2017b).*

in the ^{224}Ra SGD flux to LIS, but only a ∼6% and ∼10% decrease in the ^{226}Ra and ^{228}Ra SGD flux, respectively (total-basin mass balances). More realistic is a decrease in the ^{226}Ra and ^{228}Ra sediment diffusive flux. Many studies neglect diffusion of long-lived Ra isotopes altogether (Rama and Moore, 1996; Beck et al., 2007, 2008). Indeed, exclusion of this term would result in a 6–7% increase in the ^{226}Ra SGD flux and a 10–18% increase in the ^{228}Ra SGD flux (total-basin mass balances).

Desorption of ^{226}Ra and ^{228}Ra from resuspended sediments is assumed negligible. Desorption of ^{224}Ra from resuspended sediments is estimated to account for 14–19% of the total ^{224}Ra inventory for the total-basin mass balance. Rodellas et al. (2015) note that it is difficult to accurately constrain the Ra flux from resuspended sediments, which can be a significant Ra source in embayments with fine-grained sediments. The surface-exchangeable ^{224}Ra estimated for LIS (0.75 dpm g^{-1}) is based on shallow porewater (0–2 cm) ^{224}Ra activities from two sediment cores (Garcia-Orellana et al., 2014) and a mean K_d for Ra of 50 L kg^{-1} (Cochran, 1979; Sun and Torgersen, 2001). Even more difficult to constrain is the rate at which sediments are resuspended to release ^{224}Ra into the water column. Here, sediments are assumed to be resuspended on tidal time-scales. This term represents the second largest source of uncertainty in the ^{224}Ra mass balance (**Figure 4**). A 50% increase in the ^{224}Ra desorption flux, while keeping all other parameters equal (Eq. 1), results in a ∼14–19% decrease in the ^{224}Ra SGD flux to LIS (total-basin mass balances).

With respect to the loss by radioactive decay, the basin-wide ^{224}Ra inventory is more sensitive to this term than are the long-lived Ra inventories. Indeed, decay of ^{224}Ra dominates over mixing losses, regardless of the basin or season (**Figure 4**). This implies that a large number of water column samples are necessary to accurately capture the (near) instantaneous ^{224}Ra inventory. The ^{224}Ra inventory integrates over the half-life of ^{224}Ra, such that this inventory will accurately reflect the times of the year when the sampling was conducted, but this inventory may not be representative of a seasonal or annual ^{224}Ra flux. Importantly, this suggests that multiple sampling campaigns are necessary to capture any seasonality in the ^{224}Ra inventory for SGD flux determination. Fortunately, ^{224}Ra decay is the simplest flux term to constrain, as it is only dependent upon measuring ^{224}Ra concentration. This is the opposite case for long-lived ^{226}Ra and ^{228}Ra, where a lower number of water column samples may be adequate to capture the long-lived Ra water column inventory, while mixing terms must be well-constrained. Seasonality in long-lived Ra sources and sinks may be difficult to resolve with these isotopes because they integrate over long temporal scales.

Multiple water column Ra samples are required at the boundaries (East River and Block Island Sound in this case) to accurately constrain the boundary mixing Ra flux (**Figure 4**). The boundary water flux may be difficult to quantify in environments where numerical models or instrument deployment (e.g., ADCP) are unavailable. The ^{224}Ra inventory will be less sensitive to boundary mixing when the time-scale of mixing is sufficiently large with respect to the half-life of ^{224}Ra (**Figure 4**). Western and eastern basin long-lived Ra isotope mass balances for spring 2009 reveal that Ra sources approximately balance Ra sinks, without the need to invoke SGD. However, the uncertainties on these mass balances are quite large, owing to the uncertainty of the mixing endmember activity (East River for the western basin and Block Island Sound for the eastern basin). The Ra flux into LIS from mixing with the East River (J_{river}) and Block Island Sound (J_{in}) were each determined from one sampling station (Li et al., 1977; Turekian et al., 1996). A 50% change in the East River ^{224}Ra, ^{226}Ra, and ^{228}Ra activity, while keeping all other parameters equal (Eq. 1), results in only a 1–2% change in the ^{224}Ra SGD flux, and a 6–10% change in both the ^{226}Ra and ^{228}Ra SGD fluxes (total-basin mass balances). This is minor in comparison to the Ra flux exchanged between Block Island Sound. A 50% change in the Block Island Sound ^{224}Ra, ^{226}Ra, and ^{228}Ra activity, while keeping all other parameters equal (Eq. 1), results in only a 4–9% change in the ^{224}Ra SGD flux, but a 63–74% change in the ^{226}Ra SGD flux and a 58–60% change in the ^{228}Ra SGD flux. This highlights the critical importance of accurately determining boundary water fluxes and endmember activities, especially for the long-lived Ra isotopes (**Table 1**).

The western and eastern basin Ra activities are properly characterized (**Table 2**); thus, the central basin Ra mass balances are more adequately constrained for mixing compared to the total-basin mass balances. We emphasize that, by capturing mixing gains and losses, the central basin Ra mass balances adequately characterize the Ra-derived SGD flux, regardless of the Ra isotope used (**Figure 4**). We note that the real water exchange uncertainties may be higher than what is determined from the numerical model (**Table 1**); uncertainty in determining boundary mixing will produce large uncertainties in the long-lived Ra SGD fluxes.

The Magnitude and Significance of Submarine Groundwater Discharge to Long Island Sound

Endmember Mixing Model: An Alternative Approach to Estimate SGD

Results from the Ra mass balance in LIS reveal that SGD estimates derived from long-lived Ra isotopes are highly sensitive to boundary exchange processes (**Figure 4**). Potential uncertainties on the estimation of these boundary exchange fluxes might thus compromise the SGD estimates. An endmember mixing model

is an alternative approach to estimate the importance of SGD as a source of ^{226}Ra and ^{228}Ra to LIS, as proposed by Moore (2003). In order to simplify the system, and considering that other sources such as rivers, desorption, diffusion and decay are less important (**Figure 4**), we assume that long-lived Ra isotopes in LIS are exclusively supplied by SGD and open ocean water through boundary exchange. This approach is therefore qualitative and serves to constrain the relative magnitude of SGD only as a comparison to the mass balance. Coastal groundwater endmembers from Long Island and Connecticut shorelines have relatively distinct ^{228}Ra/^{226}Ra ratios (**Table 3** and **Figure 3**) and are thus treated as separate sources of Ra. We may thus approximate the relative contribution of Ra measured in LIS from Long Island groundwater (f_{LI}), Connecticut groundwater (f_{CT}), and seawater (f_{sea}) using a three-endmember mixing model (Moore, 2003):

$$f_{sea} + f_{LI} + f_{CT} = 1 \quad (2)$$

$$^{228}Ra_{sea} * f_{sea} + {}^{228}Ra_{LI} * f_{LI} + {}^{228}Ra_{CT} * f_{CT} = {}^{228}Ra_{measured} \quad (3)$$

$$^{226}Ra_{sea} * f_{sea} + {}^{226}Ra_{LI} * f_{LI} + {}^{226}Ra_{CT} * f_{CT} = {}^{226}Ra_{measured} \quad (4)$$

where Ra_{measured} is the measured ^{226,228}Ra activity of LIS. The three-endmember mixing model is only applied to bottom water samples from the western and eastern basins, in order to reduce riverine contributions and uncertainty in selecting a proper seawater (i.e., boundary) endmember. For the eastern basin, the seawater endmember is taken as the seasonal deep-water Ra activity of Block Island Sound. For the western basin, the seawater endmember is taken as the seasonal deep-water Ra activity of the central basin (**Table 2**). We note that the relatively large standard deviation of the endmember ^{228}Ra/^{226}Ra ratios (**Table 3**) reflects natural variability in endmember composition and thus produces considerable uncertainties in the endmember mixing models (∼30%), such that these results should be interpreted as qualitative only.

On average, Long Island groundwater contributed to 5% (spring 2009), and 6% (summer 2010) of the measured eastern basin Ra activities, with negligible contributions from Connecticut groundwater. In contrast, Long Island and Connecticut groundwaters contributed approximately equal Ra proportions to the western basin during summer 2010 (4 and 5%, respectively), while Connecticut dominated western inputs during spring 2009 (10%) with negligible inputs from Long Island. Multiplying these percentages by the volume of water in LIS (5.20×10^{13} L; **Table 4**) and dividing by a residence time of 60 days (Crowley, 2005) results in an SGD flux on the order of $\sim$1–3 $\times$ 10^{13} L y^{-1}. While this is a clear simplification of the system and thus the results can only be used in a qualitative manner, this independent approach helps constrain the relative magnitude of SGD to LIS and further helps to constrain the groundwater Ra endmember. These qualitative results demonstrate that ≥90% of the long-lived Ra isotopes in LIS are derived from boundary exchange, highlighting the critical importance of properly characterizing boundary endmembers and water exchange transports. Therefore, when boundary exchange mixing is not well constrained, it is not recommended to use ^{226}Ra and ^{228}Ra to quantify SGD in semi-enclosed basins.

SGD Volumetric Water Flow to Long Island Sound

The Ra mass balances indicate a significant amount of ^{224}Ra, ^{226}Ra, and ^{228}Ra unaccounted for, that must be balanced by inputs from SGD (**Figure 4**). The SGD Ra flux to each basin is converted into a water flow by dividing by the SGD Ra endmember activity. Results from the three-endmember mixing analysis (section "Endmember mixing model: An alternative approach to estimate SGD") reveals SGD from Connecticut is insignificant in the eastern basin and is dominated by Long Island marine groundwater; thus, Long Island groundwater is used as the Ra endmember for the eastern basin (**Table 3**). The western basin was impacted by Connecticut groundwater during spring 2009, and therefore we use the mean Connecticut marine groundwater Ra activity as an endmember during spring. In contrast, the western basin was impacted by approximately equal proportions of Long Island and Connecticut groundwater during summer 2010, and therefore an average of each endmember is used. For the central basin, we simply use an average of the Long Island and Connecticut marine groundwater Ra activities (salinity 25–28) for SGD flux determination (**Table 3**). SGD determination is highly sensitive to the selection of the groundwater endmember (Cook et al., 2018); endmember sensitivity is not evaluated in this study. Ra activities in the SGD endmembers are assumed to be constant throughout the year and therefore we only consider seasonal differences in SGD flux (Luek and Beck, 2014). Marine groundwater ^{224}Ra activities from LIS are not seasonal (Tamborski et al., 2017a), as ^{224}Ra will be quickly regenerated within shallow marine sediments, integrating all SGD flow paths. Seasonality in marine SGD to LIS may be driven, in part, by seasonal differences in density-dependent dispersive mixing within permeable sediments (Tamborski et al., 2017a), and movement of the freshwater-saltwater interface in response to regional precipitation (Michael et al., 2005; Tamborski et al., 2017b).

Volumetric SGD flows are summarized in **Figure 5**. Averaging all three Ra isotope mass balances for the total LIS basin (±standard deviation) results in an SGD flux of $1.2 \pm 0.9 \times 10^{13}$ L y^{-1} during spring 2009 and $3.8 \pm 0.7 \times 10^{13}$ L y^{-1} during summer 2010. These estimates are within the range of estimates qualitatively determined from the three-endmember mixing model and slightly lower than the ^{224}Ra-derived SGD flux of 3.2–7.4 $\times$ 10^{13} L y^{-1}, previously estimated by Garcia-Orellana et al. (2014). As noted above, the long-lived Ra isotope mass balances are significantly impacted by boundary mixing (section "Mass balance sensitivity"). The central basin Ra mass balances accurately constrain the ^{226}Ra and ^{228}Ra endmember activities of the western and eastern basins (**Table 2**), which account for the ^{226,228}Ra mixing sources and sinks, assuming that the water flow estimations are accurate (**Table 1**). The average SGD flux to the central basin of LIS is $1.1 \pm 0.8 \times 10^{13}$ L y^{-1} during spring 2009 and $1.9 \pm 0.9 \times 10^{13}$ L y^{-1} during summer 2010,

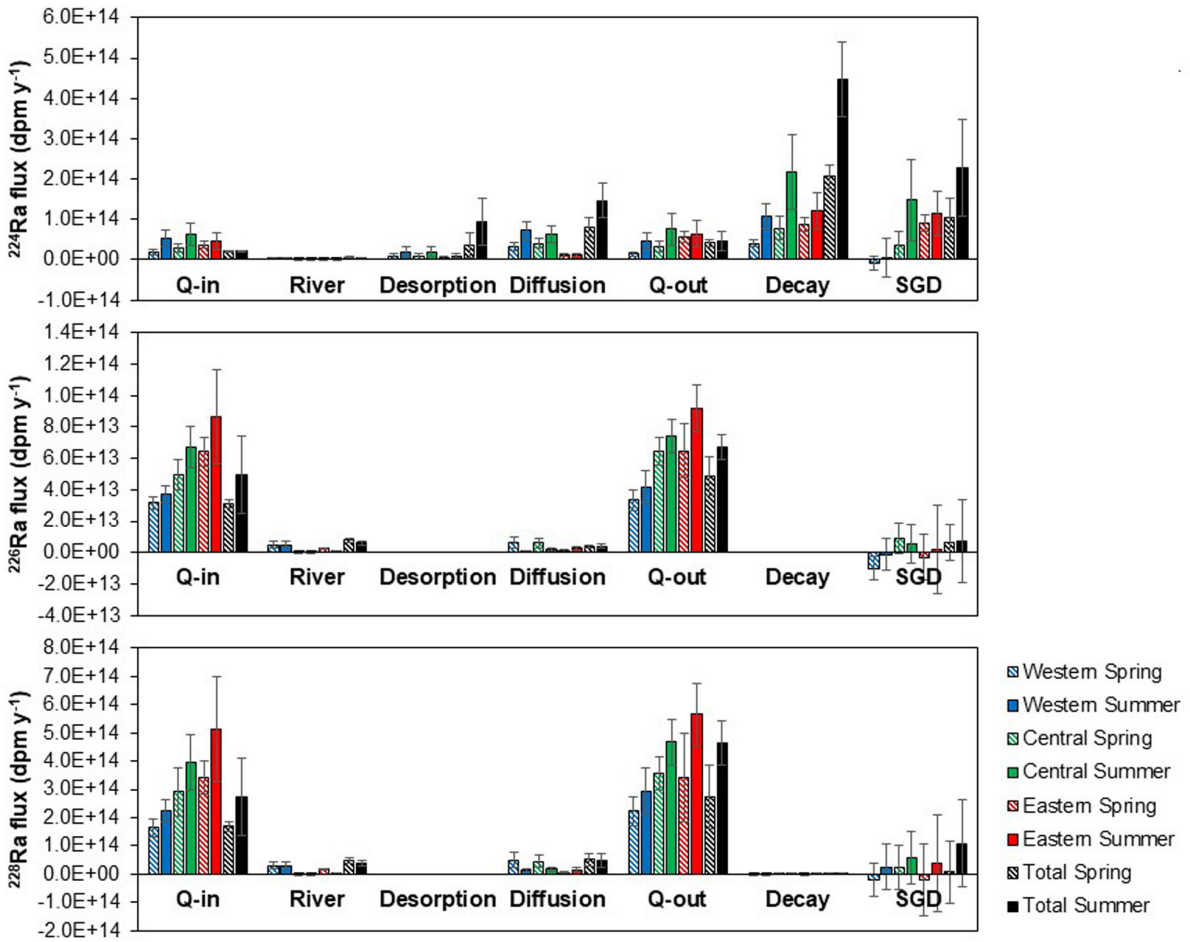

FIGURE 4 | Summary of ^{224}Ra (top), ^{226}Ra (middle), and ^{228}Ra (bottom) sources and sinks to Long Island Sound, arranged by basin and season. A negative SGD flux implies either that Ra sources approximately balance Ra sinks (within the propagated uncertainties), or that one (or more) known Ra flux is improperly characterized.

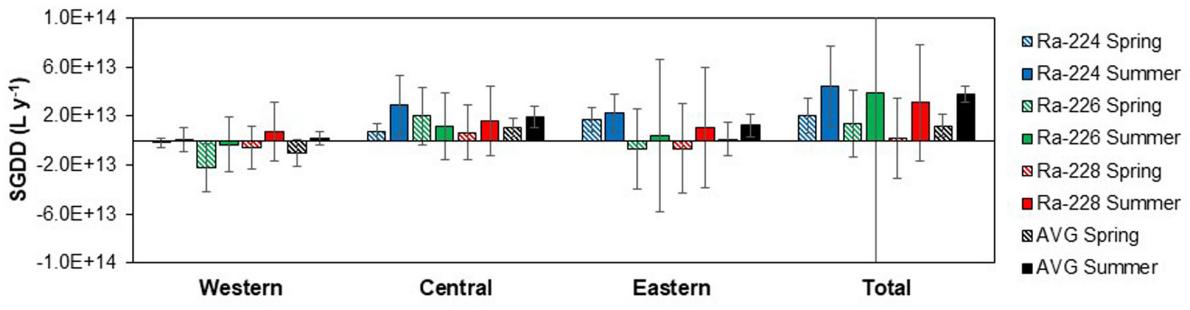

FIGURE 5 | Summary of Ra-derived SGD estimates to Long Island Sound, arranged by basin and season. The average spring and summer values (black) represent an average (±standard deviation) of all three Ra isotopes. A negative SGD flux implies either that Ra sources approximately balance Ra sinks (within the propagated uncertainties), or that one (or more) known Ra flux is improperly characterized.

or ∼50% of the SGD flux determined from the basin-wide mass balances during summer 2010. For just the central basin, the total SGD flux during spring 2009 and summer 2010 was equivalent to 45% and 280% of the freshwater inflow from the Connecticut River (2.52 and 0.68 $\times$ 10^{13} L y^{-1} during April 2009 and August 2010, respectively). Given the number of variables (Eq. 1), it is remarkable that the three different Ra isotopes converge on similar SGD values to LIS, despite relatively large uncertainties over two different seasons (**Figure 5**).

Nitrogen Loads

Excess nitrogen loading stimulates phytoplankton growth and can lead to adverse ecological conditions in LIS. Nitrogen loads from wastewater effluent and the Connecticut River are typically assumed to be the dominant sources of N to LIS (NYSDEC and CTDEP, 2000; Suffolk County, 2015). However, recent work suggests that SGD may rival the N load of wastewater effluent and rivers to LIS (Tamborski et al., 2017b). The mixing zone between groundwater and seawater in the coastal aquifer, i.e., the subterranean estuary, is critically important for controlling a variety of chemical reactions, which can add or remove chemical elements from the system (Moore, 1999). In the subterranean estuary, nitrogen in groundwater can be removed by biological processes including denitrification, or groundwater nitrogen may merely be diluted by mixing with seawater (Kroeger and Charette, 2008). Conversely, nitrate can be generated as a product of organic matter remineralization, when seawater rich in organic matter infiltrates into permeable sediments from waves and tidal forcing mechanisms. Below, we provide a revised estimate of the SGD-driven N load to LIS during spring and summer conditions, using our revised Ra isotope mass balances (**Figure 5**).

Marine SGD includes circulating seawater flow paths driven by physical forcing mechanisms, including density-driven flow and tidal pumping (Santos et al., 2012); importantly, marine SGD is separate from terrestrial (i.e., meteoric, fresh) groundwater in the ensuing analysis. Tamborski et al. (2017b) estimated a marine SGD NO_3^- endmember of 23 ± 13 μM during spring and 37 ± 29 μM during summer. This endmember is a non-conservative N enrichment, corrected for binary mixing between seawater and terrestrial groundwaters. Stable isotope analyses of $^{15}N\text{-}NO_3^-$ and $^{18}O\text{-}NO_3^-$ suggest that the marine SGD NO_3^- is derived from the remineralization of organic matter within the subterranean estuary, rather than from an atmospheric or anthropogenic source. The marine SGD flux to LIS is estimated as the total SGD flux (total-basin = $1.2 \pm 0.9 \times 10^{13}$ L y^{-1} during spring 2009 and $3.8 \pm 0.7 \times 10^{13}$ L y^{-1} during summer 2010) corrected for fresh groundwater contributions, estimated from numerical models (Scorca and Monti, 2001). As a first-order approximation, the marine SGD-driven NO_3^- flux is $2.8 \pm 2.7 \times 10^8$ mol N y^{-1} for spring 2009 and $14 \pm 11 \times 10^8$ mol N y^{-1} for summer 2010. Just considering the central basin of LIS, where SGD estimates are the most accurate (**Figure 5**), the marine SGD-driven NO_3^- flux is $2.6 \pm 2.3 \times 10^8$ mol N y^{-1} for spring 2009 and $7.1 \pm 6.4 \times 10^8$ mol N y^{-1} for summer 2010. We note that more work is required to fully constrain the spatial and temporal variability of the marine SGD NO_3^- endmember for the entire LIS basin. This first-order marine SGD NO_3^- flux is approximately two orders of magnitude greater than the N flux determined within the first 200 m of the Smithtown Bay shoreline by Tamborski et al. (2017b). Importantly, this suggests that SGD supplies a N load nearly equivalent to that of the Connecticut River and wastewater effluent, such that N loss via burial or denitrification may be greater than currently estimated (Vlahos et al., 2020). The mean annual $NO_3^- + NO_2^-$ load of the Connecticut River, measured at Middle Haddam (approximately 97% of the Connecticut River drainage area) is $4.5–4.7 \times 10^8$ mol N y^{-1}, and comprises 42–49% of the total N flux of the Connecticut River (Mullaney et al., 2018). The N load from wastewater treatment plants to LIS is approximately 5.6×10^8 mol N y^{-1} (NYSDEC and CTDEP, 2000), although this load is in decline due to improving wastewater treatment conditions (Suffolk County, 2015). Importantly, these lines of evidence suggest that far more attention should be paid to monitoring SGD-driven N loads to LIS.

CONCLUSION

Physical measurements and hydrologic models often fail to capture total SGD (Burnett et al., 2006). Ra isotopes integrate over a larger spatial area, making their use to quantify SGD a popular tool among scientists. In certain large-scale embayments like LIS, the monitoring of SGD and its associated chemical load to the sea is equally as important as monitoring riverine fluxes. However, long-term SGD monitoring is seldom performed, due to the unforeseen nature of SGD and its broad difficulty in quantification. A sensitivity analysis of Ra isotope mass balances to the semi-enclosed LIS basin reveals:

1. The selection and interpretation of the Ra isotope used will ultimately depend on the target process and flow path of interest. The different ingrowth rates of the Ra quartet enable tracing different time-scale processes. Short-lived Ra isotopes may trace short-scale length processes (Santos et al., 2012), such as wave-pumping, that are not fully captured by long-lived Ra isotopes (Rodellas et al., 2017).
2. Short-lived Ra mass balances are highly sensitive to sediment (diffusion and desorption) fluxes, but are less significantly impacted by boundary mixing (scale-dependent). When mixing is uncertain, ^{224}Ra is the preferred tracer of SGD. Studies using short-lived Ra mass balances should direct their attention toward accurately constraining sediment Ra contributions. The advantage of short-lived Ra isotopes is that their major sink is radioactive decay (scale-dependent); thus, an adequate sampling strategy can reasonably constrain the short-lived Ra inventory with minor uncertainty. Short-lived Ra mass balances can provide a reasonable first-order approximation of SGD if the Ra inventory is well-constrained and sediment contributions are minor.
3. A large number of water column samples are necessary to accurately capture the (near) instantaneous short-lived Ra inventory. The ^{224}Ra inventory integrates over the half-life of ^{224}Ra, such that this inventory will accurately reflect the times of the year when the sampling was conducted. The ^{224}Ra inventory may not be representative of a seasonal or annual ^{224}Ra flux associated with SGD, suggesting that multiple sampling campaigns are necessary to capture any seasonality in the ^{224}Ra inventory for SGD flux determination. A lower number of water column samples may be adequate to capture the long-lived Ra water column inventory; however, a greater number of samples are required to evaluate spatial variability.

4. Long-lived Ra mass balances are highly sensitive to fluxes represented by exchange at the boundaries of the system. Studies using long-lived Ra mass balances in semi-enclosed environments should direct their attention toward accurately constraining mixing gains and losses. This requires characterization of long-lived Ra activities in the inflowing and outflowing water, as well as flows of water across the boundaries. Water exchange across boundaries must be well-constrained in order to minimize the final uncertainty of the Ra SGD flux.
5. Long-term SGD monitoring using short-lived Ra isotopes will require frequent water column surveys to accurately constrain the short-lived Ra inventory. Long-term SGD monitoring using long-lived Ra isotopes should focus sampling efforts on accurately constraining mixing gains and losses.

SGD to the central basin of LIS is estimated as $1.1 \pm 0.8 \times 10^{13}$ L y^{-1} during spring 2009 and $1.9 \pm 0.9 \times 10^{13}$ L y^{-1} during summer 2010, equivalent to 45 and 280% of the freshwater inflow of the Connecticut River during the same time period. This SGD flux supplies a bioavailable N load of $2.6–7.1 \times 10^{8}$ mol N y^{-1}, similar to that of the Connecticut River (Mullaney et al., 2018). Long-term SGD monitoring is required to fully understand the magnitude and temporal variability of SGD-driven N loads to LIS.

DATA AVAILABILITY STATEMENT

All datasets generated for this study are included in the article/**Supplementary Material**.

AUTHOR CONTRIBUTIONS

JC, HB, and JG-O developed the seawater sampling strategy. JG-O, VR, JC, and CH were responsible for seawater sample collection. JT developed the groundwater sampling strategy and was responsible for groundwater and sediment core sample collection. JT, JC, JG-O, and CH were responsible for radium analyses. RW produced water exchange estimates from the model of Crowley (2005). JT developed and wrote the manuscript, with the assistance of JC, HB, JG-O, VR, CH, and RW. All authors contributed to the article and approved the submitted version.

FUNDING

This project has been funded by New York Sea Grant projects (R/CCP-16 and R/CMC-12). This research is contributing to the ICTA-UAB Unit of Excellence "María de Maeztu" (MDM-2015-0552) and MERS (2017 SGR – 1588, Generalitat de Catalunya). VR acknowledges financial support from the Beatriu de Pinós postdoctoral program of the Catalan Government (2017-BP-00334).

ACKNOWLEDGMENTS

We thank David Bowman and the crews of the R/V *Seawolf* for their assistance in sampling.

SUPPLEMENTARY MATERIAL

The Supplementary Material for this article can be found online at: https://www.frontiersin.org/articles/10.3389/fenvs.2020.00108/full#supplementary-material

TABLE S1 | Summary of Ra isotope mass balances, arranged by basin and season.

REFERENCES

Beck, A. J., Rapaglia, J. P., Cochran, J. K., and Bokuniewicz, H. J. (2007). Radium mass-balance in Jamaica Bay, NY: evidence for a substantial flux of submarine groundwater. *Mar. Chem.* 106, 419–441. doi: 10.1016/j.marchem.2007.03.008

Beck, A. J., Rapaglia, J. P., Cochran, J. K., Bokuniewicz, H. J., and Yang, S. (2008). Submarine groundwater discharge to Great South Bay, NY, estimated using Ra isotopes. *Mar. Chem.* 109, 279–291. doi: 10.1016/j.marchem.2007.07.011

Bokuniewicz, H. (1980). Groundwater seepage into Great South Bay, New York. *Estuar. Coast. Mar. Sci.* 10, 437–444. doi: 10.1016/S0302-3524(80)80122-8

Bokuniewicz, H., Cochran, J. K., Garcia-Orellana, J., Valenti, R., Wallace, D. J., Christina, H., et al. (2015). Intertidal percolation through beach sands as a source of 224,223Ra to Long Island Sound, New York and Connecticut, United States. *J. Mar. Res.* 73, 123–140. doi: 10.1357/002224015816665570

Burnett, W. C., Aggarwal, P. K., Aureli, A., Bokuniewicz, H., Cable, J. E., Charette, M. A., et al. (2006). Quantifying submarine groundwater discharge in the coastal zone via multiple methods. *Sci. Total Environ.* 367, 498–543. doi: 10.1016/j.scitotenv.2006.05.009

Buxton, H. T., and Modica, E. (1992). Patterns and rates of groundwater flow on Long Island. New York. *Ground Water* 30, 857–866. doi: 10.1111/j.1745-6584.1992.tb01568.x

Cai, P., Shi, X., Moore, W. S., Peng, S., Wang, G., and Dai, M. (2014). 224Ra:228Th disequilibrium in coastal sediments: implications for solute transfer across the sediment-water interface. *Geochim. Cosmochim. Acta* 125, 68–84. doi: 10.1016/j.gca.2013.09.029

Capone, D. G., and Bautista, M. F. (1985). A groundwater source of nitrate in nearshore marine sediments. *Nature* 313, 214–216. doi: 10.1038/313214a0

Charette, M. A., Moore, W. S., and Burnett, W. C. (2008). "Uranium- and thorium-series nuclides as tracers of submarine groundwater discharge," in *U-Th Series Nuclides in Aquatic Systems*, eds S. Krishnaswami, and J. K. Cochran, (Amsterdam: Elsevier), 155–192.

Cochran, J. K. (1979). *The Geochemistry of 226Ra and 228Ra in Marine Deposits*. Ph.D. Thesis, Yale University, New Haven, CT.

Cook, P. G., Rodellas, V., and Stieglitz, T. (2018). Quantifying surface water, porewater and groundwater interactions using tracers: tracer fluxes, water fluxes, and end-member concentrations. *Water Resour. Res.* 54, 2452–2465. doi: 10.1002/2017WR021780

Copenhaver, S. A., Krishnaswami, S., Turekian, K. K., Epler, N., and Cochran, J. K. (1993). Retardation of 238U and 232Th decay chain radionuclides in Long Island and Connecticut aquifers. *Geochim. Cosmochim. Acta* 57, 597–603. doi: 10.1016/0016-7037(93)90370-c

Crowley, H. (2005). *The Seasonal Evolution of Thermohaline Circulation in Long Island Sound*. Ph.D. thesis, Stony Brook University, Stony Brook, NY.

Dion, E. P. (1983). *Trace Elements and Radionuclides in the Connecticut River and Amazon River Estuary*. Ph.D. Thesis, Yale University, New Haven, CT.

Garcia-Orellana, J., Cochran, J. K., Bokuniewicz, H., Daniel, J. W. R., Rodell, V., Heilbrun, C., et al. (2014). Evaluation of 224Ra as a tracer for submarine groundwater discharge in Long Island Sound (NY). *Geochim. Cosmochim. Acta* 141, 314–330. doi: 10.1016/j.gca.2014.05.009

Garcia-Solsona, E., Masqué, P., Garcia-Orellana, J., Rapaglia, J., Beck, A. J., Cochran, J. K., et al. (2008). Estimating submarine groundwater discharge around Isola La Cura, northern Venice Lagoon (Italy), by using the radium quartet. *Mar. Chem.* 109, 292–306. doi: 10.1016/j.marchem.2008.02.007

Jia, Y., and Whitney, M. W. (2019). Summertime Connecticut River Water Pathways and Wind Impacts. *JGR Oceans* 124, 1897–1914. doi: 10.1029/2018JC014486

Knee, K. L., Crook, E. D., Hench, J. L., Leichter, J. J., and Paytan, A. (2016). Assessment of submarine groundwater discharge (SGD) as a source of dissolved radium and nutrients to Moorea (French Polynesia) coastal waters. *Estuar. Coasts* 39, 1651–1668. doi: 10.1007/s12237-016-0108-y

Knee, K. L., and Paytan, A. (2011). "Submarine groundwater discharge: a source of nutrients, metals and pollutants to the coastal ocean," in *Treatise on Estuarine and Coastal Science*, Vol. 4, eds E. Wolanski, and D. S. McLusky (Waltham: Academic Press), 205–233.

Koppelman, L. E., Weyl, P. K., Gross, M. G., and Davies, D. S. (1976). *Urban Sea: Long Island Sound*. Westport, CT: Praeger Publishers.

Krishnaswami, S., Graustein, W. C., and Turekian, K. K. (1982). Radium, thorium and radioactive lead isotopes in groundwaters: application to the in situ determination of adsorption-desorption rate constants and retardation factors. *Water Resour. Res.* 18, 1633–1675.

Kroeger, K. D., and Charette, M. A. (2008). Nitrogen biogeochemistry of submarine groundwater discharge. *Limnol. Oceanogr.* 53, 1025–1039. doi: 10.4319/lo.2008.53.3.1025

Latimer, J., Tedesco, M., Swanson, R., Yarish, C., Stacey, P., and Garza, C. (2013). *Long Island Sound: Prospects for the urban sea*. Berlin: Springer.

Li, Y.-H., Mathieu, G., Biscaye, P., and Simpson, H. J. (1977). The flux of 226Ra from estuarine and continental shelf sediments. *Earth Planet. Sci. Lett.* 37, 237–241. doi: 10.1016/0012-821x(77)90168-6

Luek, J. L., and Beck, A. J. (2014). Radium budget of the York River estuary (VA, USA) dominated by submarine groundwater discharge with a seasonally variable groundwater end-member. *Mar. Chem.* 165, 55–65. doi: 10.1016/j.marchem.2014.08.001

Michael, H. A., Mulligan, A. E., and Harvey, C. F. (2005). Seasonal oscillations in water exchange between aquifers and the coastal ocean. *Nature* 436, 1145–1148. doi: 10.1038/nature03935

Moore, W. S. (1999). The subterranean estuary: a reaction zone of ground water and sea water. *Mar. Chem.* 65, 111–125. doi: 10.1016/S0304-4203(99)00014-6

Moore, W. S. (2003). Sources and fluxes of submarine groundwater discharge delineated by radium isotopes. *Biogeochemistry* 66, 75–93. doi: 10.1023/B:BIOG.0000006065.77764.a0

Moore, W. S. (2010). "The effect of submarine groundwater discharge on the ocean," in *Annual Review of Marine Science*, (Palo Alto: Annual Reviews), 59–88.

Moore, W. S., and Arnold, R. (1996). Measurement of Ra-223 and Ra-224 in coastal waters using a delayed coincidence counter. *J Geophys Res* 101, 1321–1329. doi: 10.1029/95JC03139

Moore, W. S., Blanton, J. O., and Joye, S. B. (2006). Estimates of flushing times, submarine groundwater discharge, and nutrient fluxes to Okatee Estuary, South Carolina. *J. Geophys. Res.* 111:C090006. doi: 10.1029/2005JC003041

Mullaney, J. R., Martin, J. W., and Morrison, J. (2018). *Nitrogen Concentrations and Loads for the Connecticut River at Middle Haddam, Connecticut, Computed with the use of Autosampling and Continuous Measurements Of Water Quality for Water Years 2009 to 2014*. U.S. Geological Survey Scientific Investigations Report 2018–5006. (Reston, VI: USGS), doi: 10.3133/sir20185006

NYSDEC and CTDEP (2000). *A Total Maximum Daily Load Analysis to Achieve Water Quality Standards for Dissolved Oxygen in Long Island Sound*. Albany, NY: NYSDEC, 55.

Poppe, L. J., Knebel, H. J., and Mlodzinska, Z. J. (2000). Distribution of surficial sediment in Long Island Sound and adjacent waters: texture and total organic carbon. *J. Coast Res.* 16, 567–574.

Rama, and Moore, W. S. (1996). Using the radium quartet for evaluating groundwater input and water exchange in salt marshes. *Geochim. Cosmochim. Acta* 60, 4645–4652. doi: 10.1016/s0016-7037(96)00289-x

Rodellas, V., Garcia-Orellana, J., Garcia-Solsona, E., Masqué, P., Domínguez, J. A., Ballesteros, B. J., et al. (2012). Quantifying groundwater discharge from different sources into a Mediterranean wetland by using 222Rn and Ra isotopes. *J. Hydrol.* 466–467, 11–22. doi: 10.1016/j.jhydrol.2012.07.005

Rodellas, V., Garcia-Orellana, J., Masqué, P., and Font-Muñoz, J. S. (2015). The influence of sediment sources on radium-derived estimates of submarine groundwater discharge. *Mar. Chem.* 171, 107–117. doi: 10.1016/j.marchem.2015.02.010

Rodellas, V., Garcia-Orellana, J., Trezzi, G., Masque, P., Steiglitz, T. C., Bokuniewicz, H., et al. (2017). Using the radium quartet to quantify submarine groundwater discharge and porewater exchange. *Geochim. Cosmochim. Acta* 196, 58–73. doi: 10.1016/j.gca.2016.09.016

Santos, I. R., Eyre, B. D., and Huettel, M. (2012). The driving forces of porewater and groundwater flow in permeable coastal sediments: a review. *Estuar. Coast. Shelf Sci.* 98, 1–15. doi: 10.1016/j.ecss.2011.10.024

Scorca, M. P., and Monti, J. (2001). *Estimates of Nitrogen Loads Entering Long Island Sound from Ground Water and Streams on Long Island, New York, 1985-96*. Coram, N.Y: U.S. Dept. of the Interior, U.S. Geological Survey.

Shi, X., Mason, R. P., and Charette, M. A. (2018). Mercury flux from salt marsh sediments: Insights from a comparison between 224Ra/228Th disequilibrium and core incubation methods. *Geochim. Cosmochim. Acta* 222, 569–583. doi: 10.1016/j.gca.2017.10.033

Suffolk County (2015). *Suffolk County Comprehensive Water Resources Management Plan*. Reston, VI: USGS.

Sun, Y., and Torgersen, T. (2001). Adsorption-desorption reactions and bioturbation transport of ^{224}Ra in marine sediments: a one-dimensional model with applications. *Mar. Chem.* 74, 227–243. doi: 10.1016/S0304-4203(01)00017-2

Swarzenski, P. W. (2007). U/Th series radionuclides as coastal groundwater tracers. *Chem. Rev.* 107, 663–674. doi: 10.1021/cr0503761

Tamborski, J. J., Cochran, J. K., and Bokuniewicz, H. J. (2017a). Application of 224Ra and 222Rn for evaluating seawater residence times in a tidal subterranean estuary. *Mar. Chem.* 189, 32–45. doi: 10.1016/j.marchem.2016.12.006

Tamborski, J. J., Cochran, J. K., and Bokuniewicz, H. J. (2017b). Submarine groundwater discharge driven nitrogen fluxes to Long Island Sound, NY: terrestrial vs. marine sources. *Geochim. Cosmochim. Acta* 218, 40–57. doi: 10.1016/j.gca.2017.09.003

Turekian, K. K., Tanaka, N., and Turekian, V. C. (1996). Transfer rates of dissolved tracers through estuaries based on 228Ra: a study of Long Island Sound. *Cont. Shelf Res.* 16, 863–873. doi: 10.1016/0278-4343(95)00039-9

Vlahos, P., Whitney, M. M., Menniti, C., Mullaney, J. R., Morrison, J., and Jia, Y. (2020). Nitrogen budgets of the Long Island Sound estuary. *Estuar. Coast. Shelf Sci.* 232:10693. doi: 10.1016/j.ecss.2019.106493

Conflict of Interest: The authors declare that the research was conducted in the absence of any commercial or financial relationships that could be construed as a potential conflict of interest.